University of Baghdad
College of Engineering
JOURNAL OF ENGINEERING

Journal of Engineering
journal homepage: www.joe.uobaghdad.edu.iq
Number 1 Volume 27 January 2021

Civil and Architectural Engineering

Finite Element Analysis of Cracked One-Way Bubbled Slabs Strengthened By External Prestressed Strands

Falah Hassan Ibrahim*
Ph.D. student
College of engineering
Baghdad/Iraq
Falahhassan425@gmail.com

Ali Hussein Ali Al-Ahmed
Assist Prof.
College of engineering
Baghdad/Iraq
Dr.Ali-Alahmed@coeng.uobaghdad.edu.iq

ABSTRACT

Bubbled slabs can be exposed to damage or deterioration during its life. Therefore, the solution for strengthening must be provided. For the simulation of this case, the analysis of finite elements was carried out using ABAQUS 2017 software on six simply supported specimens, during which five are voided with 88 bubbles, and the other is solid. The slab specimens with symmetric boundary conditions were of dimensions 3200/570/150 mm. The solid slab and one bubbled slab are deemed references. Each of the other slabs was exposed to; (1) service charge, then unloaded (2) external prestressing and (3) loading to collapse under two line load. The external strengthening was applied using prestressed wire with four approaches, which are L1-E, L2-E, L1-E2, and L2-E2, where the lengths and eccentricities of prestressed wire are (L1=1800, L2=2400, E1=120 and E2=150 mm). The results showed that each reinforcement approach restores the initial capacity of the bubbled slab and improves it in the ultimate load capacity aspect. The minimum and maximum ultimate strength of strengthened cracked bubbled slab increased by (17.3%-64.5%) and (25.7%-76.3%) than solid and bubbled slab, respectively. It is easier to improve behavior with an increased eccentricity of the prestressed wire than to increase its length.

Keywords: Bubbled slabs, Strengthening, Prestressing, Finite element analysis.

*Corresponding author
Peer review under the responsibility of University of Baghdad.
https://doi.org/10.31026/j.eng.2021.01.04

Article received: 14/7/2020
Article accepted: 18 / 9/2020
Article published:1/1/2021

تحليل السقوف المتشققة أحادية الاتجاه ذات الفقاعات و المقواة خارجيا بواسطة الجدائل مسبقة الجهد و ذلك باستخدام نظرية العناصر المحددة

فلاح حسن ابراهيم
طالب دكتوراه
قسم الهندسة المدنية
كلية الهندسة/جامعة بغداد

علي حسين علي ال احمد
أستاذ مساعد
قسم الهندسة المدنية
كلية الهندسة/جامعة بغداد

الخلاصة

قد تتعرض السقوف الفقاعية الى التدهور أو التلف خلال فترة وجودها في المنشأ مما يستوجب اجراء المعالجات لتقويتها. وعليه تم تمثيل هذه المشكلة و حلها بالاعتماد على نظرية العناصر المحددة و باستخدام برنامج ABAQUS2017 .تمت نمذجة ستة نماذج أحدهما لسقف خالي من الفقاعات و خمسة أخريات ذات فقاعات بعدد 88 فقاعة بنفس القطر و التوزيع .أبعاد النموذج هي 3200x570x150ملم و قطر الفقاعة 100 ملم و كانت المسافة بين مراكز الفقاعات بالاتجاه الطولي و العرضي هي 140ملم . تم اعتبار النموذج الخالي من الفقاعات و أحد النماذج الخمسة كسقوف مرجعية للمقارنة , بينما تم تعريض النماذج الأربعة المتبقية الى الحمل الخدمي ثم أزالة هذا الحمل ومن ثم تقويتها باستخدام الأسلاك الخارجية مسبقة الجهد و أخيرا تم تحميلها حتى الفشل التام. المتغيرات الأساسية في التقوية الخارجية كانت طول السلك و مستواه عن مركز السقف الفقاعي حيث كانت التقويات الأربعة هي (L1−E1,L2−E1,L1−E2 and L2−E2) حيث ,L1=1800,L2=2400,E1=120 (E2=150) ملم. أظهرت النتائج أن كل انواع التقوية قد حسنت التصرف العام و القدرة النهائية للسقوف الفقاعية المقواة في مرحلة الخدمة حيث كانت أقل و أكبر زيادة مقارنة بنموذج السقف الخالي من الفقاعات و السقف ذو الفقاعات (17,3%−64,5%) و (25,7%−76,3%) على التوالي. وان زيادة مستوى الأسلاك مسبقة الجهد أكثر فعالية في التقوية مقارنة بزيادة طول السلك .

1. INTRODUCTION

The method of finite elements is based on the thought that each system is physically composed of varied components, and thus its solution could even be represented in parts. Moreover, the solution is represented over each part as a linear combination of undetermined parameters and known position, and possibly time functions. The shape, material properties, and physical behavior of the parts can differ from each other.

Even if the system has one geometric shape and consists of one material, representing its solution in a piece-wise manner is simpler. There are basically two nonlinearity sources: geometric and material. The geometrical nonlinearity is created purely from geometrical consideration (i.e., nonlinear strain-displacement relationship). The second material nonlinearity is attributable to nonlinear constitutive material behavior. A third type may arise due to variation in initial or boundary conditions **(Reddy, 2004).**

ABAQUS is also used to study simple structural problems (stress/displacement). It really can simulate problems in specific, numerous contexts as heat transfer, mass diffusion, electrical component thermal management (coupled thermal-electrical analysis), acoustics, soil mechanics (coupled pore fluid stress analysis) as well as piezoelectrical analysis **(ABAQUS, 2016).** The mathematical formulation of physical problems supported assumptions that certain quantities may be neglected may reduce the matter to a linear one. Linear solutions are simple and have fewer computational costs than nonlinear solutions.

There are many numerical analyzes of conventional bubbled slabs with various parameters such as slab thickness, bubble diameter and configuration, top and bottom longitudinal reinforcement, etc. The findings of a numerical study conducted by **(Bindea, et al., 2015)** showed even under a longitudinal reinforcement rate of less than 0.50 percent, flat slabs containing spherical voids do not struggle to shear force, and over this amount, the effective shear force declines compared to solid slabs also as the rate of reinforcement increases.

A numerical investigation (Pandey and Srivastava, 2016) evaluated the highest moment and shear force by applying the 100kN moving load on the bubble deck slab and the solid deck slab. The results indicated that, under the same conditions, the maximum moments, shear force with in-plan stress in the bubble deck were 10-25 percent below that of the solid concrete slab. A study of finite elements on the voided 100 mm thick slab and varied spacing of void formers was done. Results showed they tend to behave exactly like a solid slab as the slab's spacing increases **(Subramanian and Bhuvaneshwari, 2015).**

Very few theoretical studies have adopted the strengthening of bubbled slabs using FRP such as **(Jasna, and Vishnu, 2018; Reshma, and Binu, 2015; 2016)**. An experimental and theoretical study conducted by **(Oukaili and Yasseen, 2015)** investigated the effect of internal strengthening using initial pre-tensioning strands on the general behavior of one-way bubbled slabs in aspects of deformation and ultimate load. The results viewed that the partially prestressed strengthening enhanced the previous aspects.

For strengthening of reinforced concrete T-beam using external post-tensioning technique with different lengths and eccentricities of prestressed strands, research by (**Said, et al., 2015)** showed that this technique increased the ultimate capacity of the strengthened beams and reduced the deflection and strains a same stage of loading.

As per a review of the literature that included experimental and numerical research papers to strengthen just one way bubbled slab during serviceability, it is often said that this numerical study might even be the primary one in this field. One loading stage is simulated for ordinary solid and bubbled slabs, and three for strengthening.

The major parts of a bubbled deck slab are six in this study: concrete blocks, reinforcing steel bars and anchor bolts embedded inside the concrete, upper steel plate under monotonic loading, lower steel plate as boundary conditions, and upper and lower stiffener steel plates for external reinforcement.

2.NUMERICAL WORK

2.1 General

If conducted with appropriate boundary conditions and material properties, the finite element method will provide in-depth knowledge about member's behavior. The obstacle of accomplishing FEA is time-consuming, and getting properties of materials for patterns of crack propagation can also be a complex process. Slabs that consume plenty of the concrete in any structure require only a smaller amount of concrete to carry all the hundreds applied to them. Therefore the inactive concrete, which is usually in the core zone, will have to be removed to optimize the concrete slab consumption. Since the concrete used is reduced, the slab's self-weight and therefore, the entire structure is reduced.

2.2 Material Modeling of Concrete

ABAQUS / Standard does have three models for concrete behavior; smeared cracking, brittle concrete cracking model, and damaged plasticity. Attributable to the oriented concepts of damaged elasticity, the constitutive calculations are affected by the crack. These concepts are administered after failure cracking to elucidate the material reaction's reversible neighborhood **(Chaudhari and Chakrabarti, 2012).** However, due to the convergence problems that may be caused by the non-existence of cyclic/unloading response or the damage within the elastic stiffness likely to result from plastic strain **(Daud, 2015).** It is difficult to make the model suitable for 3D applications. Also, the damaged plasticity model is used in structures undergoing dynamic or cyclic loading due to the potential for anticipating the test's behavior to failure **(Rusinowski, 2005).** For the above reasoning, the damage plasticity model was used during serviceability to analyze the strength of cracked bubbled deck slabs.
The damage parameters can range from zero (characterizing the undamaged material) to at least one (characterizing total loss of force). The default plasticity of injury is often illustrated using **Fig. 1**.

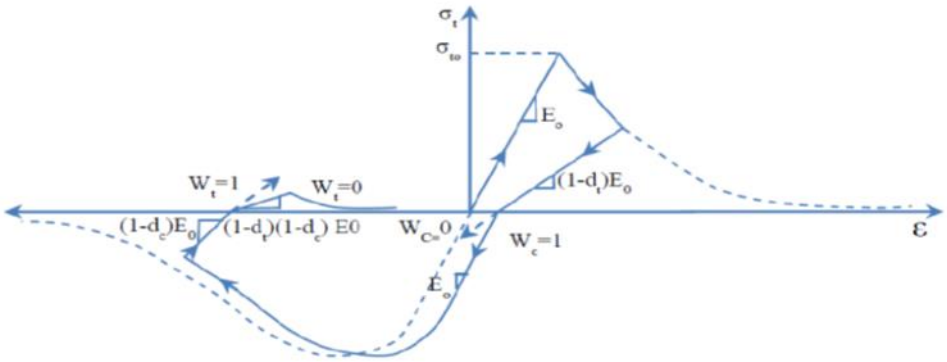

Figure 1. Uniaxial load cycle (tension-compression-tension), **(ABAQUS, 2011).**

2.2.1 Plasticity parameters

The five parameters required for definition are:

ψ is the dilation angle where it represents the proportion of the quantity modification to shear strain. ε, a parameter referenced as flow potential eccentricity, ε_{bo} /ε_{co} is that the proportion of initial equibiaxial compressive strength to initial uni-axial compressive strength. μ is the viscosity parameter that represents the viscoplastic recovery time and typically aims to enhance the convergence speed of the slab model in the softening region. It is presumed to be zero, so the slab model won't cause severe convergence complexity.

Consequently, within the present research, no viscoplastic regularization is conducted, and Kc is that the ratio of the second stress invariant to the tensile meridian (T.M.) thereto to the compressive meridian (C.M.) and it represents the yield surface in deviator plane, as shown in **Fig. 2** And this should satisfy $0.5 < Kc < 1.0$

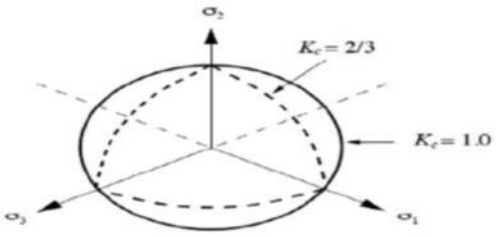

Figure 2. Yield surfaces in the deviatoric plane, corresponding to different values of *Kc* **(ABAQUS, 2011).**

2.2.2 Compressive behavior

Just after the elastic region, the uniaxial compressive stress-strain relationship for plain concrete must be defined. According to ABAQUS, the ranges of hardening as well as strain softening are expressed in terms of compressive stress, $\sigma_c$and elastic strain$\tilde{\epsilon_c}^{in}$. Throughout this research, the finite element method identified the uniaxial concrete model **(British Standards, 2004, Eurocode 2).**

2.2.3 Tensile behavior

There are three main approaches available in ABAQUS/standard to understand the post cracking tension softening curve by identifying strain, crack opening (displacement) or fracture energy, as seen in **Fig. 3**. The relationship of tensile stress-strain softening, supported strength criterion could introduce mesh sensitivity within the causes of plain concrete (**Abdullah and Bailey, 2010).**

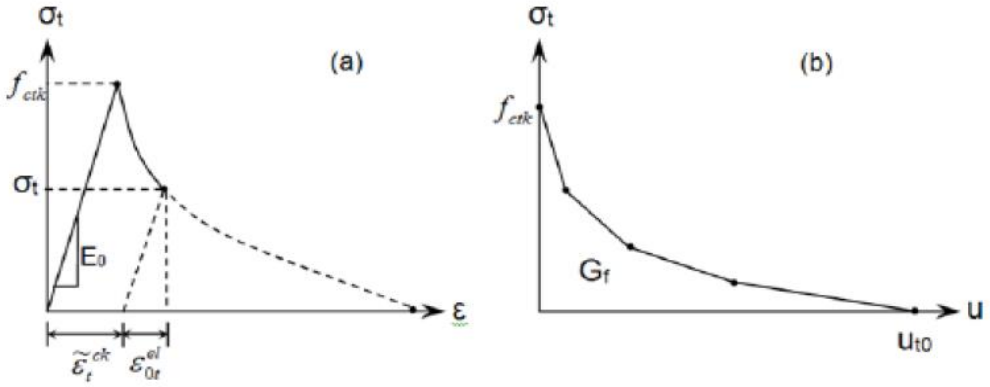

(a) stress-strain approach (b) fracture

Figure 3. Post-failure tensile behavior **(Abdullah and Bailey, 2010).**

2.2.4 Tension stiffening model

Because the cracked concrete will initially carry some tensile stresses within the normal direction of the crack due to the concrete and steel reinforcement interaction, the tension stiffening effect is taken into account. This will be done by assuming that the concrete stress component normal to the cracked plane is gradually released. Tension stiffening models supported strength criteria represented by three curves within the current analysis: linear, bilinear, and exponential curves. **(Wang and Hsu, 2001)**, obtained the graph shown in **Fig. 4**.

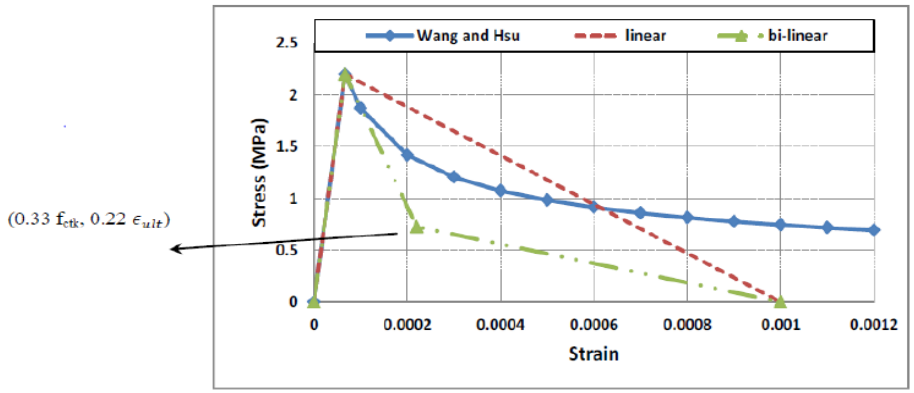

Figure 4. Uniaxial tensile stress-strain behavior of concrete **(Wang and Hsu, 2001).**

2.3 Input Data

In **Figs. 5, and 6,** all required parameters such as strength f_{cu}, Youngs Modulus, and stress-strain curve data points are shown. For several other parameters needed, including the dilation angle, the eccentricity$\epsilon_{bo}/\epsilon_{co}, k_c$. The viscosity parameter, the default data of ABAQUS or on the brink of it are shown in **Tables 1, 2, and 3**.

Table 1. Concrete compressive strength data.

Yield Stress (MPa)	Inelastic Strain	Yield Stress (MPa)	Inelastic Strain	Yield Stress (MPa)	Inelastic Strain	Yield Stress (MPa)	Inelastic Strain
21.20087	0	40.5	0.001605685	39.24266	0.00216637	35.54865	0.002799856
26.44987	0.000336036	40.47399	0.001681193	38.86145	0.002252491	34.82862	0.002896099
30.83082	0.000486717	40.39619	0.001758249	38.43085	0.002340087	34.06146	0.002993751
34.36694	0.000662638	40.26696	0.001836841	37.95121	0.002429149		
37.08067	0.000863131	40.08665	0.00191696	37.42284	0.002519666		
38.99362	0.001087549	39.8556	0.001998594	36.84608	0.002611629		
40.12668	0.001335267	39.57416	0.002081734	36.22124	0.002705029		

Table 2. Concrete tension stiffening.

Yield Stress (MPa)	Cracking strain
3	0
0.1	0.01

Table 3. Input material data for concrete plasticity.

Youngs modulus	24000
Poissons ratio	0.15
Dilation angle	36
Eccentricity	0.1
$\epsilon_{bo}/\epsilon_{co}$	1.16
k_c	0.667
Viscosity parameter	0

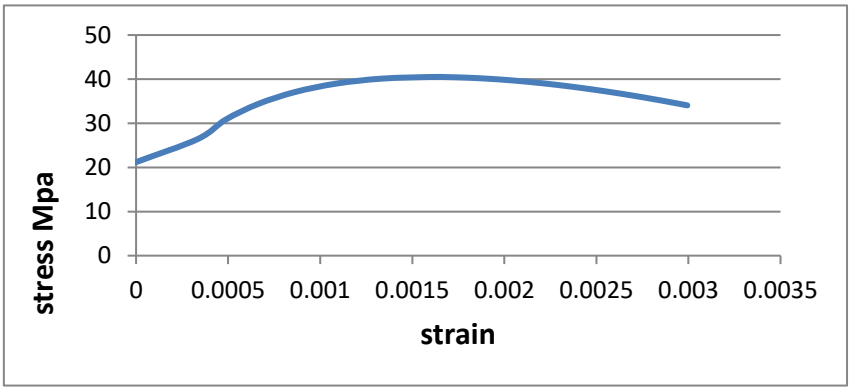

Figure 5. Uniaxial compressive stress-strain behavior of concrete.

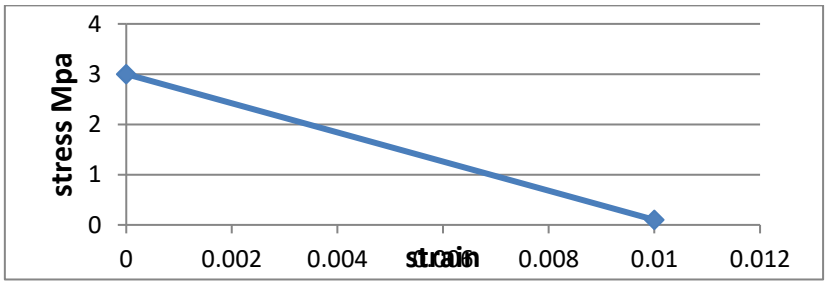

Figure 6. Uniaxial tensile stress-strain behavior of concrete.

2.3.1 Steel components

Fig. 7 illustrates steel compressive uniaxial and tensile stress-strain behavior. Besides, steel reinforcement is used in the classical plasticity model for elastoplastic hardening material supported by steel. **Table 4** shows the true stress input and true strain used in this analysis.

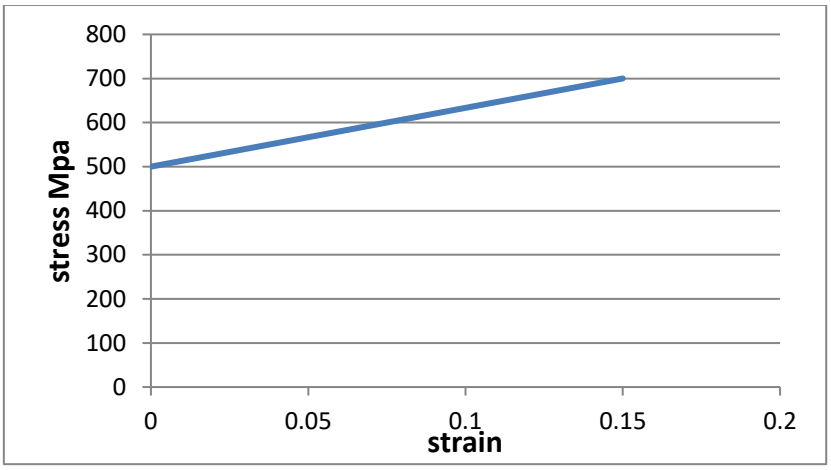

Figure 7. Uniaxial compressive and tensile stress-strain behavior of steel.

Table 4. The input value of stress, strain, and modulus of elasticity.

Steel components	Stress	Strain	Modules of elasticity
Rebar	500 700	0 0.15	200000

2.4 Element Types and Interaction

The bubbled deck slabs are modeled in three dimensions, which are modeled using standard 3D stress elements for all components except the reinforcements. These elements provided the acceptable rules of integration, which embraced the specimen's experimental response. Reinforcement is most often modeled using elements such as solid, beam, or truss. The use of solid elements is computationally costly, and therefore not selected. Because the reinforcing bars do not provide a really high bending rigidity, truss elements are used and modeled as an embedded element. It is assumed that their contact with the concrete is perfectly bonded. The reinforcement slip is often patterned by modifying concrete behavior. This is not studied within the current work, however. For the modeling of solid concrete slabs, an 8-node linear brick (C3D8R) element is used. The element tends to be not stiff enough in bending and stress, strains within the integration points are the most accurate. The C3D8R element integration point is located within the middle of the element. Therefore small elements are required at the boundary of a structure to capture a stress concentration. The same brick element (C3D8R) is used in the modeling of steel sheets under line

pressure, steel boundary support sheets, anchor bolts, and the upper and hence the upper and lower steel sheets for strengthening. A 4 node linear brick (C3D4) tetrahedron element is used for concrete bubbled slabs to indicate an adequate representation between solid and voided concrete masses.

On the other hand, a linear 3D two-node truss element with three degrees of freedom at each node (T3D2) is used for the embedded reinforcement bars. **Fig. 8** Shows the element of 8-node brick and 4-node tetrahedron with integration point. Solid spheres with a radius (100 mm) are made and moved to the right positions within the solid slab block and, by subtracting all the solid spheres from the solid slab, the voids are to be formed within the cross-section center.

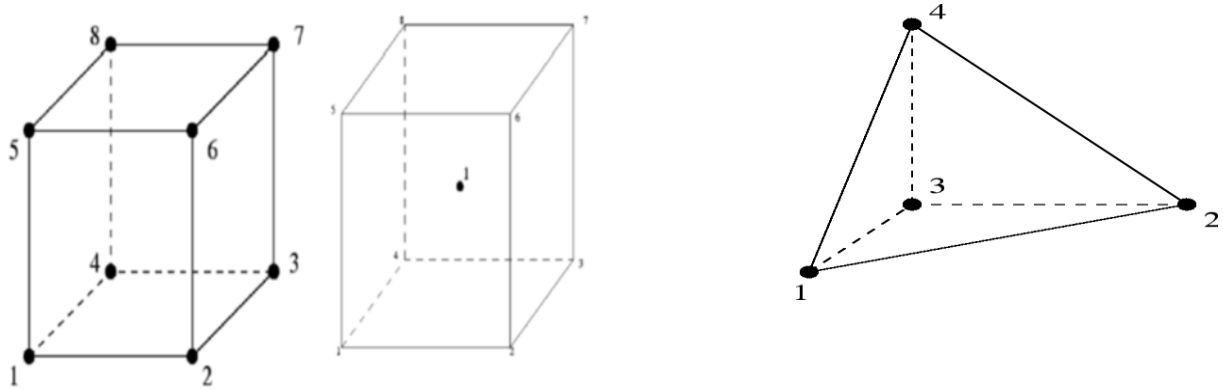

(a): 8-node brick element with integration point (b): tetrahedron element

Figure 8. Brick and Tetrahedron Elements.

The formulation of the finite interaction elements introduced in the modeling is based primarily on the kinematic method: interaction without penetration and conditions of friction are described kinematically at the nodes. Individuals expressed in terms of force and displacement.

2.5 Boundary Conditions

The slabs had been tested with simple supports for all the specimens. One support provided both vertical and longitudinal displacements (directions y and z) with restrictions while enabling rotations around (x-axis), (hinge support). The second support restricted only vertical displacements (direction y) whilst still allowing longitudinal displacements and rotations around the x-plane axis (roller support).

2.6 Modeling of Applied Load

The loading conditions were simulated in ABAQUS, using the load step process, as two line load on models during tests. The effective length (L), width (B), and height (H) of solid and bubbled slabs are 3000,570 and 150 mm, respectively. The total length is 3200 mm. The force was modeled as loading pressure to avoid the exposure of concrete elements to the high concentrated stresses that result in early cracking, resulting in early divergence in the analysis. The distance between the charging of two lines is 800 mm. The distance between the two prestressed wires is 300 mm. For the simulation of external prestressed force (30 kN) within each wire, the approach of applying the action of this force within the specific nodes is adopted instead of prestressed wire simulation.

2.7 Meshing of the Model

Analysis of finite elements requires model meshes. In ABAQUS, the mesh module process contains capabilities that help the meshes' auto-generation on the created parts and assemblies. Two kinds of meshes are used during this study: one for solid slabs and one for bubbled slabs.

2.8 Modeling of Solid Slab

Fig. 9 illustrates the top and bottom steel meshes of all solid slabs consist of 8 bars ø10 mm as longitudinal reinforcement and 44 bar ø 10 mm as shrinkage and temperature reinforcement in the transversal direction.

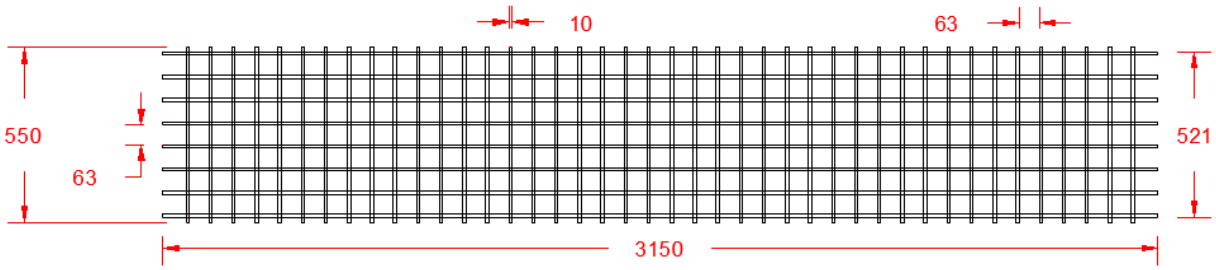

Figure 9. Longitudinal and Transversal Reinforcement .

One simulation for the solid slab is adopted, as shown in plate 1, according to what has been mentioned previously.

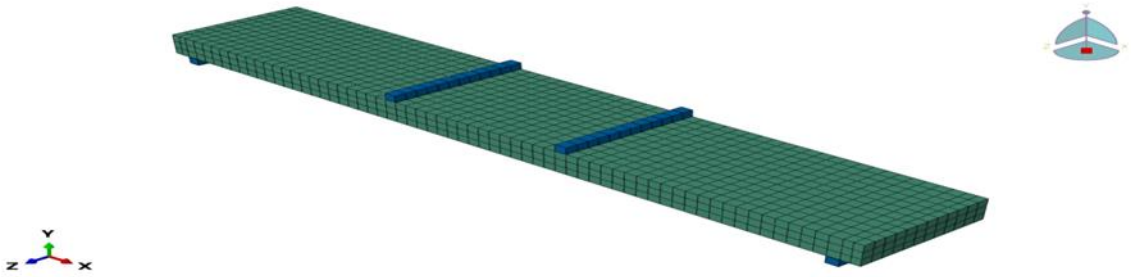

Plate 1. Solid slab SD with brick element mesh.

2.9 Modeling of Bubbled Slabs

Fig. 10 shows the diameter, transversal, and longitudinal arrangements of spherical voids in all bubbled slabs. The bubble (D) diameter is 100 mm, and the center to center distance between bubbles in transversal and longitudinal directions(S) is 140 mm. Same top and bottom meshes of reinforcement of SD are used in bubbled slab BD with rearrangement of bars due to insert bubbles.

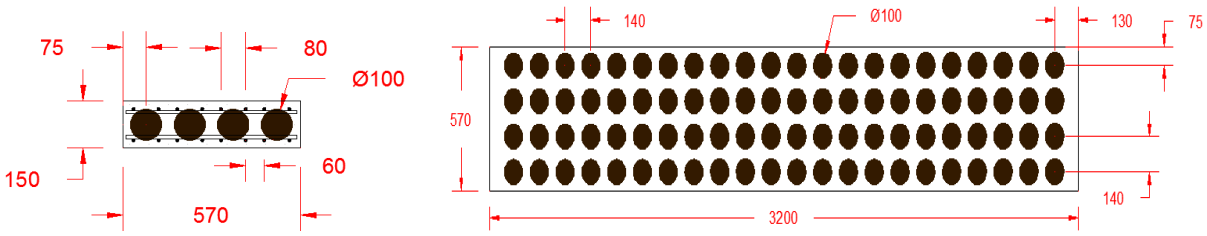

Figure 10. Longitudinal and Transversal Arrangements of Voids in Bubbled Slabs.

To achieve the aims of this study, all the bubbled slabs are simulated in the same way as shown in **plates 2 and 3**.

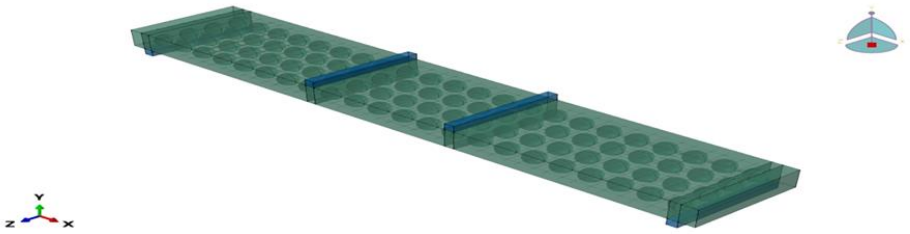

Plate 2. Isometric see-through view of bubbled slab BD.

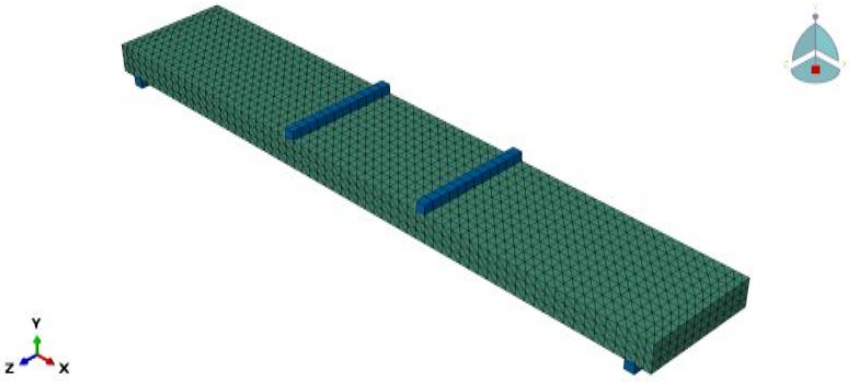

Plate 3. BD bubbled slab with tetra mesh.

2.10 Modeling of Strengthen Cracked Bubbled Deck Slab BD

Because the; (1)simulation of the reinforcement of any cracked bubbled deck slab is the same for all bubbled specimens,(2) the purpose of numerical analysis using the ABAQUS program is to guide the potential of this program both in simulation and in case study resolution, the bubbled deck slab BD is chosen to be reinforced with four approaches L1-E1, L2-E1, L1-E2, and L2-E2. In this study, L1 and L2 are lengths of prestressed wires, and E1 and E2 are the eccentricity of them (distance from the level of prestressed wires to the center of the slab). L1=1800mm, L2= 2400mm (short and long prestressed wire, E1=120mm, and E2=150 mm (small and large eccentricity of prestressed wire). The ratios of L1/L, L2/L are 0.6, 0.8(strengthening ratios), and

E1/H and E2/H are 0.8 and 1.0 (depth ratios). Like previously mentioned, each approach has three stages of loading;(1) loading BD to just the service limit (0.6Pu), after that unloading,(2) going to apply prestressed force in each wire(30KN) is a type of pre-loading action,(3) reloading again till collapse**. Plates 4-6** show the specimen BD with the strengthening equipment required.

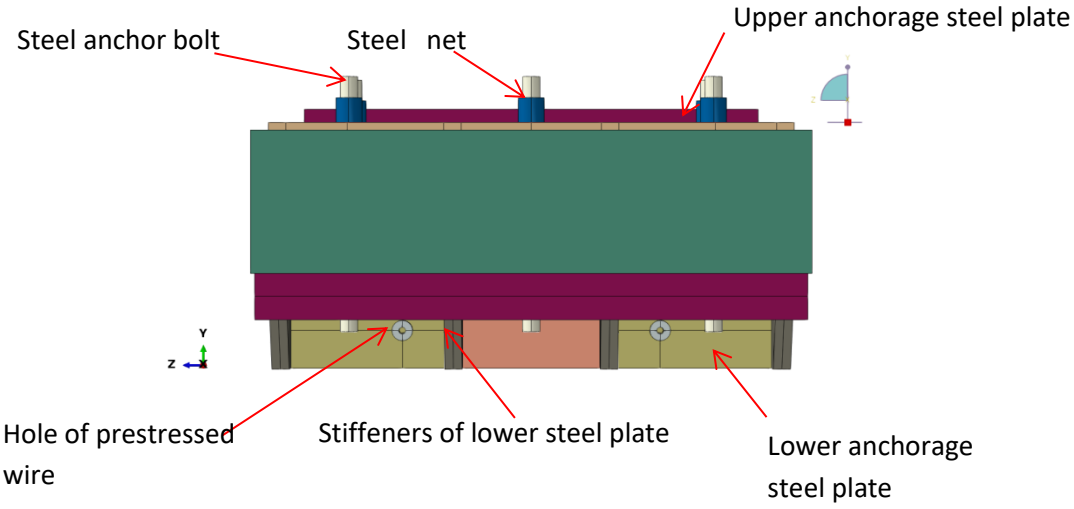

Plate 4. Side view in upper and lower anchorage stiffener steel plates.

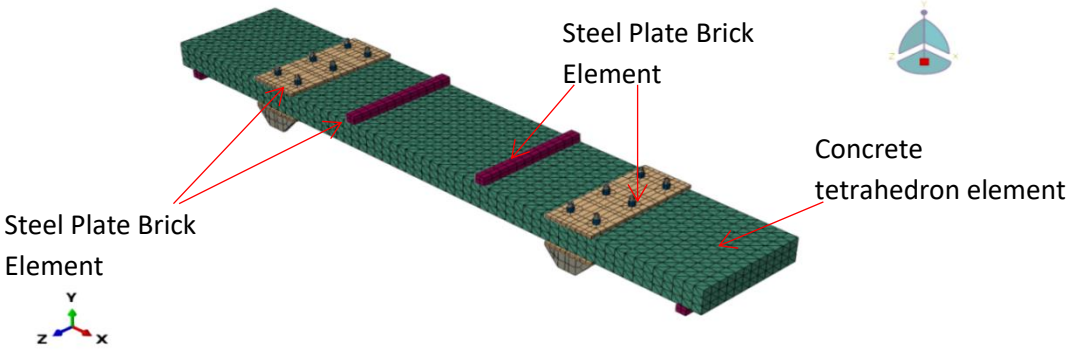

Plate 5. Tetra meshing of strengthening of the cracked bubbled slab.

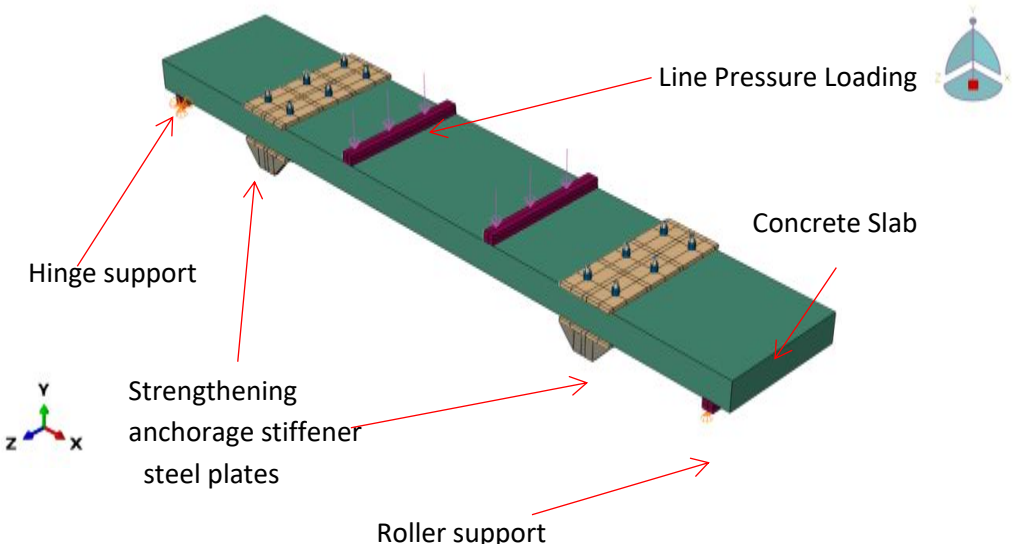

Plate 6. Isometric view of the cracked bubbled slab during applied load.

3. RESULTS AND DISCUSSIONS

3.1 General

The evaluation of finite elements is conducted to understand the performance of load-deflection, cracking behavior (maximum plastic principal strains), damage plasticity, and Von-Mises stresses both for solid as well as voided slabs in longitudinal reinforcing steel.

3.2 Load vs. Deflection Behavior

The voided slabs behaved almost like the solid slab, but there was an increase within the deflection values. The justification is that the decline within a member's stiffness is due to concrete abolition. On the other hand, there are several reasons why the finite-element models will cause the upper stiffness. First, micro-cracks produced by drying shrinkage and handling that are present up to a point within the concrete. The particular specimens' stiffness could be significant, while the finite element models do not include micro-cracks.

Second, in the finite-element analysis, the right bond between concrete and reinforcing steel is assumed, but the idea would not be true for the specific specimens. **Fig.11** shows the idealization of three load-deflection response stages of strengthening cracked bubbled slab.

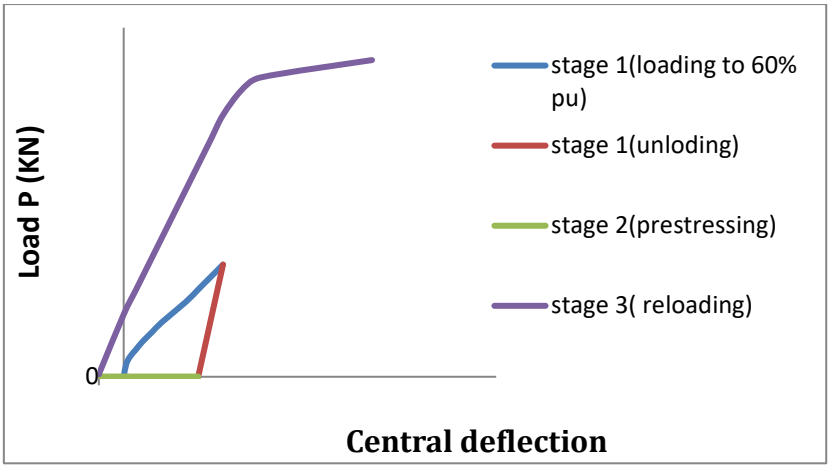

Figure 11. The idealization of Load-Deflection of strengthening of the cracked bubbled deck slab.

Fig.12 illustrates the load-deflection response of SD, BD, BD-L1-E1, BD-L2-E1, BD-L1-E2, and BD-L2-E2. It is evident that the bubbled slab BD shows an increase in deflection than SD and all other models at the same loading stage due to a reduction in BD stiffness resulting from inserting voids inside the slab core. On the contrary, the cracked bubbled slab's strengthening with four strengthening approaches L1-E1, L2-E1, L1-E2, and L2-E2 increased the upward deflection (camber), respectively. The ultimate load and deflection of the reinforced cracked bubbled slab with any reinforcement approach increased than conventional solid and bubbled slabs, as shown in **Table 5**. It is evident that increasing prestressed eccentricity is more effective in increasing the ultimate load rather than increasing the length of prestressed wire.

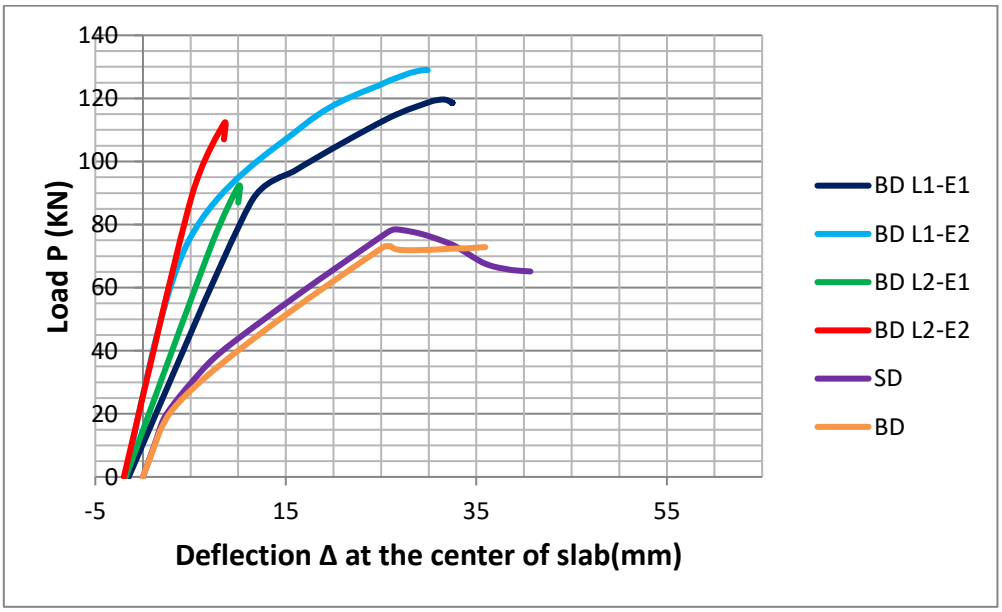

Figure 12. Load vs. Deflection by FEA of all models.

Table 5. Ultimate camber, load, and displacement and mode of failure of all models.

Model	Camber (mm)	S/B ratio	D/H ratio	Strengthening ratio	Depth ratio	Ultimate strength (kN)	Ultimate displacement (mm)	Failure mode
SD	---------- ---	---	---	---	---	78.4	26.75	Flexural Failure
BD	---------- ---	0.24	0.67	---	---	73.15	25.34	Flexural Failure
BD-L1-E1	1.5	0.24	0.67	0.6	0.8	121.35	31.9	Flexural Failure
BD-L2-E1	1.8	0.24	0.67	0.8	0.8	92	10	Shear-Failure
BD-L1-E2	1.9	0.24	0.67	0.6	1	129	29.78	Flexural Failure
BD-L2-E2	2.0	0.24	0.67	0.8	1	112	8.5	Shear-Failure

It is clear that the cambering increased with increasing length and eccentricities of prestressed wire. Also, the ultimate strength of solid model SD is larger than BD by 7.1% due to insert the bubbles in the core of the slab, which reduces the stiffness of the bubbled section.
From **Table 5**, it is evident the minimum and maximum ultimate strength increased than solid and bubbled slab by (17.3%-64.5%) and (25.7%-76.3%) respectively. The ABAQUS software succeeds in simulating and modeling the problem and solution of the cracked bubbled section.

The final deflection and cambering of all models are obtained. For the briefing, some models as examples are given in **plates** 7-**10.**

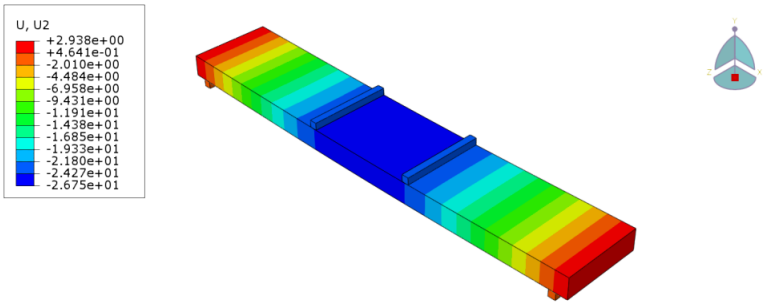

Plate 7. Deflection of solid slab SD.

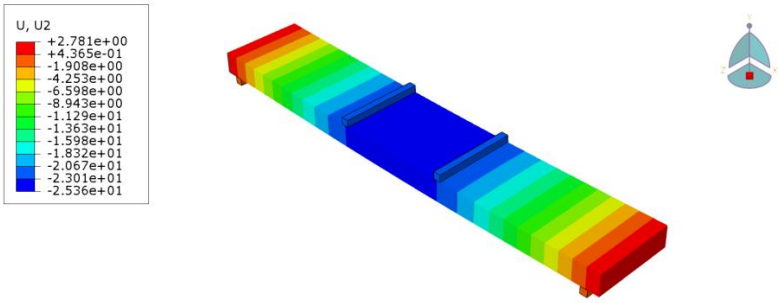

Plate 8. Deflection of bubbled slab BD.

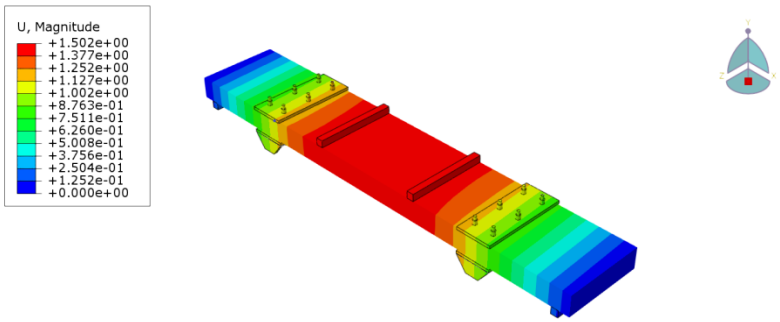

Plate 9. Cambering of strengthened cracked bubbled slab BD-L1-E1.

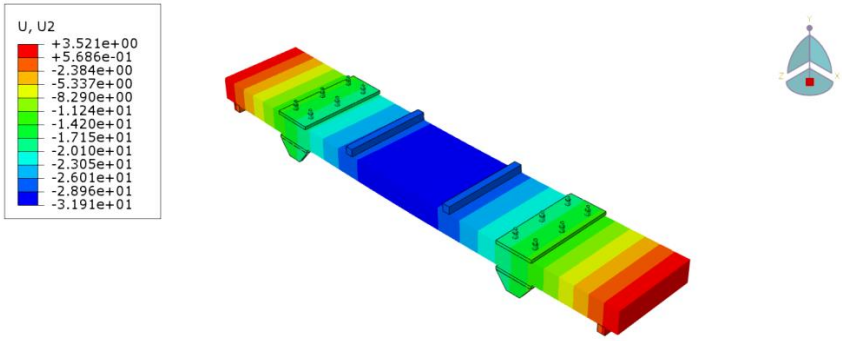

Plate 10. Deflection of strengthened cracked bubbled slab BD-L1-E1.

3.3 Maximum principal plastic strain

Maximum plastic stress in the tension zone is an indication of cracking when the tensile strain exceeds the ultimate concrete tensile strength. The maximum main plastic strain is provided for all models, as shown in **plates 11-16**.

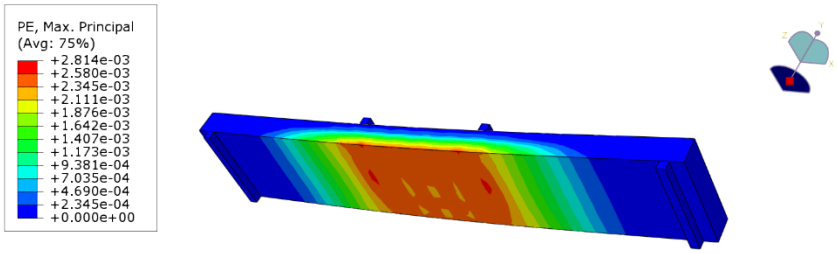

Plate 11. Maximum principal plastic strain of solid slab SD.

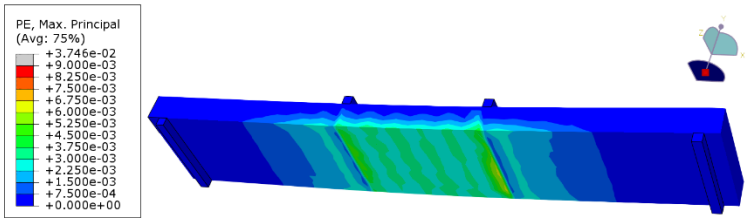

Plate 12. Maximum principal plastic strain of bubbled slab BD.

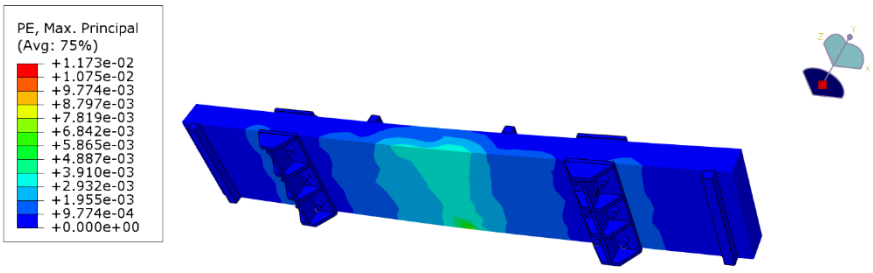

Plate 13. Maximum principal plastic strain of strengthened cracked bubbled slab BD-L1-E1.

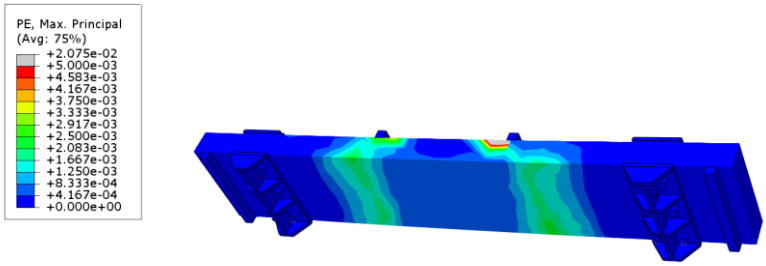

Plate 14. Maximum principal plastic strain of strengthened cracked bubbled slab BD-L2-E1.

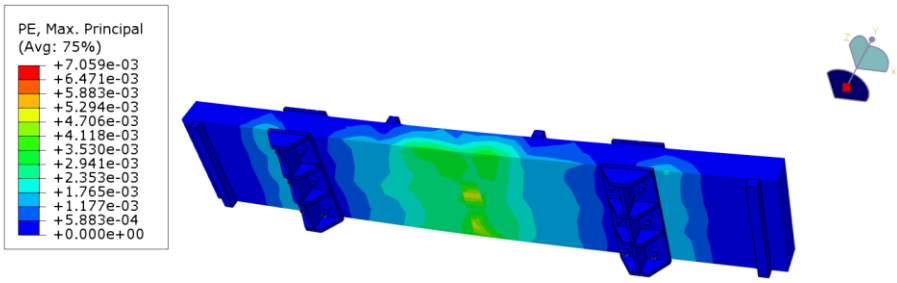

Plate 15. The maximum principal plastic strain of strengthened cracked bubbled slab BD-L1-E2.

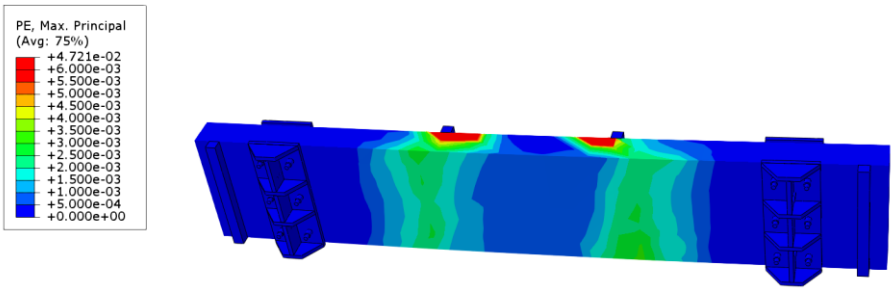

Plate 16. The maximum principal plastic strain of strengthened cracked bubbled slab BD-L2-E2.

3.4 Damage plasticity index

In **plates 17-21**, the Damage plasticity index of models as examples is shown. This index represents the percentage of material property losses that occur at failure.

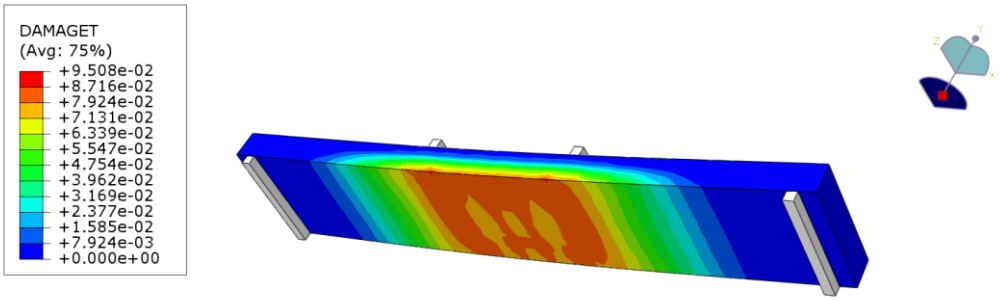

Plate 17. Damage plasticity index of solid slab SD.

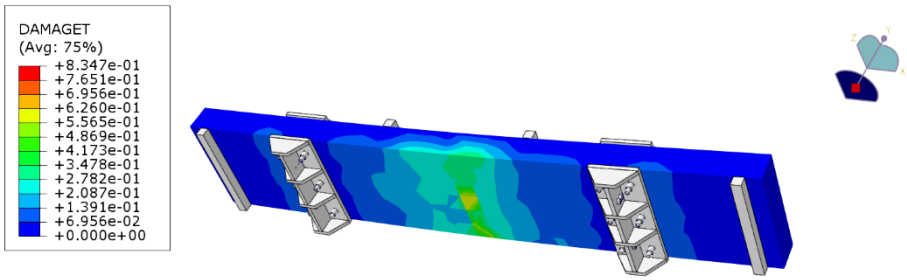

Plate 18. Damage plasticity index of strengthened cracked bubbled slab BD-L1-E1.

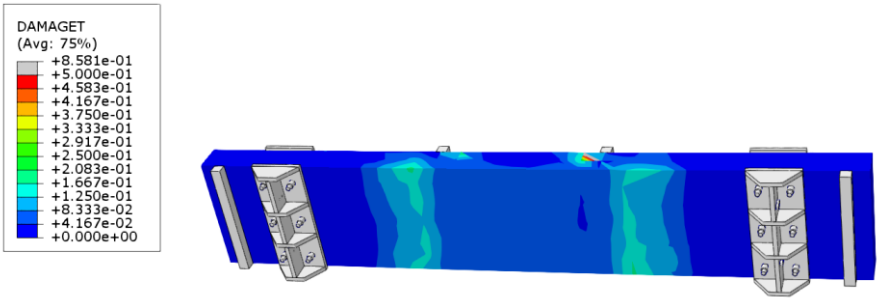

Plate 19. Damage plasticity index of strengthened cracked bubbled slab BD-L2-E1.

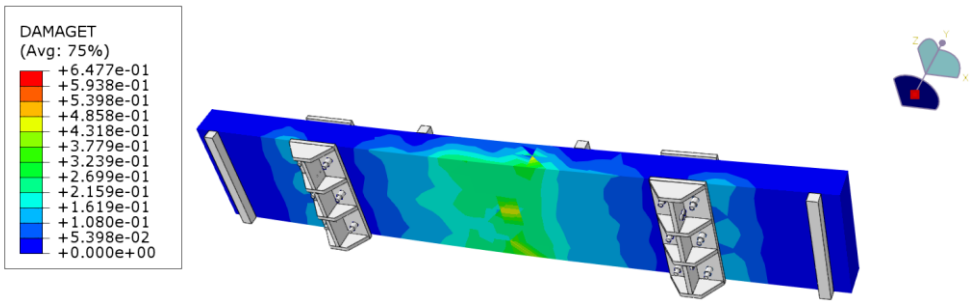

Plate 20. Damage plasticity index of strengthened cracked bubbled slab BD-L1-E2.

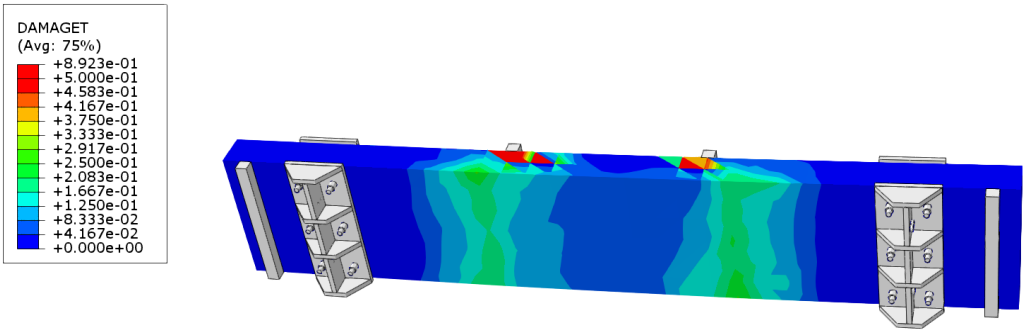

Plate 21. Damage plasticity index of strengthened cracked bubbled slab BD-L2-E2.

3.5 Von- Mises Stress

According to the finite element analysis results, the bottom longitudinal reinforcement reached the assumed yield point for all models that failed in flexural failure mode at the mid-span. **Plate 22,** for example, shows this for BD-L1-E2.

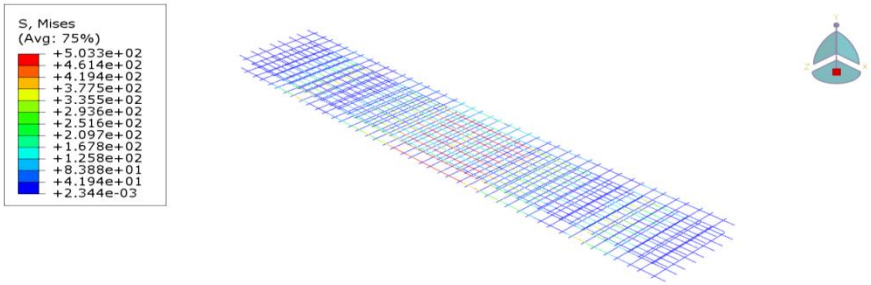

Plate 22. Von - Mises stress of BD-L1-E2 model.

4. CONCLUSIONS

The above finite element study was performed on the conventional solid and voided slabs and strengthening of cracked bubbled slabs during serviceability with same S/B ratio=0.24and D/H ratio= 0.67 by four approaches of external strengthening associated with length and eccentricity of prestressed wires (two strengthening ratios 0.6 and 0.8 and two depth ratios 0.8 and 1). According to the finite element results, the conclusions are:

- The conventional bubbled slab showed an increase in deflection rather than a solid slab at the same stage of loading due to the reduction of its stiffness resulting from eliminating concrete from the slab core. Also, the ultimate load of a bubbled slab decrease than a solid slab by 6.6%

This finite element study's main aim is achieved by using an external post-tensioning technique to strengthen cracked bubbled deck slabs.

- The applying of external strengthening in stage two has closed the initial flexural cracks of the first stage; thereby, the bubbled section restored its ultimate strength and enhanced it.
- The conventional bubbled and solid slabs showed an increase in deflection at the same stage of loading rather than any strengthened slabs.
- The stiffness of the strengthened cracked bubbled slabs increased with increasing the strengthening ratio from 0.6 to 0.8. Also, the stiffness increased when the depth ratio increased from 0.8 to 1.
- The minimum and maximum ultimate strength of the strengthened slabs increased than solid and bubbled slabs by (17.3%-64.5%) and (25.7%-76.3%) respectively.
- Increase the eccentricity of prestressed wire (depth ratio) is more effective in increasing the ultimate load than increasing the length of prestressed wire (strengthening ratio). In other words, using the strengthening ratio 0.6 with depth ratios 0.8 and 1 are better than using the strengthening ratio 0.8 with depth ratios 0.8 and 1.
- The highest ultimate strength is achieved by using strengthening ratio 0.6 and depth ratio 1.
- All the models failed in flexural failure mode after yielding bottom longitudinal reinforcement except the models strengthened by strengthening ratio of 0.8 with both depth ratios of 0.8 and 1which failed in shear mode. In other words, the failure mode changed from flexure to shear when the strengthening ratio changed from 0.6 to 0.8. This may be due to extend the length of prestressed wires more than an acceptable limit in the shear zone (strengthening ratio 0.8) and the second-order effects.
- ABAQUS software succeeds in modeling the specific problem of cracked bubbled section and the solution of its strengthening.

REFERENCES

- ABAQUS, CAE., 2011. Users manual. ABAQUS analysis users manual.
- ABAQUS, CAE., 2016. 6.14.1, help.
- Abdullah, A. M., and Bailey, C. G., 2010. Analysis of repaired/strengthened RC structures using composite materials: punching shear. *University of Manchester.*
- Bindea, M., Chezan, C. M., and Puskas, A., 2015. Numerical analysis of flat slabs with spherical voids subjected to shear force. *Journal of Applied Engineering Sciences, 5*(1), pp.7-13.
- Chaudhari, S. V., and Chakrabarti, M. A., 2012. Modeling of concrete for nonlinear analysis using finite element code ABAQUS. *International Journal of Computer Applications, 44*(7), pp.14-18.
- Daud, R. A., 2015. Behaviour of reinforced concrete slabs strengthened externally with two-way FRP sheets subjected to cyclic loads. *The University of Manchester (United Kingdom).*

- Jasna Jamal., and Vishnu. Vijayan., 2018. A Study on strengthening bubble deck slab with elliptical balls using GFRP Sheets, *International Journal for scientific research and development IJSRD* vol. 6.

- Oukaili, N. K. A., and Yasseen, H. H., 2015. Theoretical Investigations on the Structural Behavior of Biaxial Hollow Concrete Slabs. *Journal of Engineering*, *21*(6), pp.108-130.

- Pandey, M., and Srivastava, M., 2016. Analysis of bubble deck slab design by finite element method. *IJSTE-International Journal of Science Technology and Engineering*, *2*(11).

- Reddy, J. N., 2004. An Introduction to Nonlinear Finite Element Analysis, *Texas, Oxford University Press.*

- Reshma. Mathew. Binu. P., 2015. CFRP Strips on punching shear strength development of bubble deck slab. *International journal of advanced research trends in engineering and technology. IJARTET*, vol. 2.

- Reshma. Mathew. Binu. P., 2016. Punching shear strength development of bubble deck slab using GFRP stirrups, *International conference on emerging trends in engineering and management ICETEM*.

- Rusinowski, P., 2005., Two-way concrete slabs with openings: experiments, finite element analyses and design.

- Said, A. I., Al-Ahmed, A. H. A., and Al-Fendawy, D. M., 2015. Strengthening of Reinforced Concrete T-Section Beams Using External Post-Tensioning Technique. *Journal of Engineering*, *21*(12), pp.139-154.

- Standard, B., 2004. Eurocode 2: Design of concrete structures—. *Part 1-1:* General rules and rules for buildings, p.230.

- Subramanian, K., and Bhuvaneshwari, P., 2015. Finite element analysis of voided slab with high density polypropylene void formers. *International Journal of Chem Tech Research, CODEN (USA): IJCRGG ISSN*, pp.0974-4290.

- Wang, T., and Hsu, T. T., 2001. Nonlinear finite element analysis of concrete structures using new constitutive models. *Computers & structures*, *79*(32), pp.2781-2791.